nature neuroscience

APC^{Cdh1} mediates EphA4-dependent downregulation of AMPA receptors in homeostatic plasticity

Amy K Y Fu, Kwok-Wang Hung, Wing-Yu Fu, Chong Shen, Yu Chen, Jun Xia, Kwok-On Lai & Nancy Y Ip

Homeostatic plasticity is crucial for maintaining neuronal output by counteracting unrestrained changes in synaptic strength. Chronic elevation of synaptic activity by bicuculline reduces the amplitude of miniature excitatory postsynaptic currents (mEPSCs), but the underlying mechanisms of this effect remain unclear. We found that activation of EphA4 resulted in a decrease in synaptic and surface GluR1 and attenuated mEPSC amplitude through a degradation pathway that requires the ubiquitin proteasome system (UPS). Elevated synaptic activity resulted in increased tyrosine phosphorylation of EphA4, which associated with the ubiquitin ligase anaphase-promoting complex (APC) and its activator Cdh1 in neurons in a ligand-dependent manner. APC^{Cdh1} interacted with and targeted GluR1 for proteasomal degradation *in vitro*, whereas depletion of Cdh1 in neurons abolished the EphA4-dependent downregulation of GluR1. Knockdown of EphA4 or Cdh1 prevented the reduction in mEPSC amplitude in neurons that was a result of chronic elevated activity. Our results define a mechanism by which EphA4 regulates homeostatic plasticity through an APC^{Cdh1}-dependent degradation pathway.

Neurons adjust their excitability in response to changes in the strength and number of synapses. This form of synaptic scaling is a homeostatic response that is believed to prevent unconstrained changes in synaptic strength during development and learning, and is essential for maintaining the stability of the neuronal network[1]. Pharmacological blockade of neuronal activity by tetrodotoxin (TTX) or elevation of synaptic activity by the $GABA_A$ receptor antagonist bicuculline leads to compensatory changes in synaptic strength, as revealed by an increase or decrease in mEPSC amplitude, respectively[2]. The molecular mechanisms that underlie these homeostatic responses are beginning to be identified. The reduction in mEPSC amplitude that follows chronic exposure to bicuculline involves downregulation of surface AMPA receptors (AMPARs) at synapses[2–4]. There is emerging evidence that synaptic scaling after prolonged elevated activity also depends on the UPS[5,6].

The UPS enzymes E1 (activating enzyme), E2 (conjugating enzymes) and E3 (ligases) act sequentially to add the 76 amino-acid peptide ubiquitin to target proteins. Mono-ubiquitination modulates the function of protein substrates by regulating protein-protein interactions or endocytosis[7]. By contrast, addition of polymeric ubiquitin (polyubiquitination) to target proteins leads to their degradation by proteasomes[8]. Immunocytochemical analysis of cultured neurons has shown that both ubiquitin and proteasomes are found at synapses[9,10]. Components of the UPS are also present in biochemical preparations of the postsynaptic density[11,12]. Interestingly, polyubiquitination and the subsequent degradation of postsynaptic proteins are bidirectionally regulated during chronic treatment of dissociated neurons with TTX and bicuculline[13], which suggests that the UPS has an important role in adjusting the molecular composition of synapses during homeostatic plasticity. In *Drosophila* and *Caenorhabditis elegans*, the ubiquitin ligases APC and Skp1/Cul1/F-box protein (SCF) regulate the accumulation of synaptic glutamate receptors[14–16]. Surface expression of AMPARs in rodent hippocampal neurons, which is regulated in different forms of neuronal plasticity, also depends on the ubiquitination and proteasome-mediated degradation of postsynaptic scaffold proteins such as PSD-95 (refs. 10,17). However, a recent study has indicated that AMPARs themselves undergo proteasome-dependent degradation[18]. It is unclear whether and how the proteasome-mediated degradation of AMPARs is regulated in mammalian neurons during synaptic scaling.

Eph receptors and their membrane-bound ligands (ephrins) have well-established functions in various developmental processes[19], and there is emerging evidence that ephrins and Eph receptors are important for synaptic plasticity and learning[20]. For example, mice lacking EphB2 and ephrin-B ligands show impaired long-term potentiation (LTP), and disruption of EphB-ephrinB interaction attenuates the induction of LTP at mossy fiber-CA3 synapses. EphA4 knockout mice also show defective LTP in the amygdala[21]. However, the mechanism that underlies the role of Eph receptors in synaptic plasticity remains unclear. One plausible mechanism might involve modifications in the growth and morphology of dendritic spines. Whereas EphA4 has a crucial role in the retraction of dendritic spines[22,23], activation of EphB receptors promotes dendritic spine formation[24,25]. EphB receptors also directly interact with NMDA receptors (NMDARs) and enhance Ca^{2+} influx and CREB-mediated transcription induced by NMDA during synapse formation[26,27]. The significance of such cross-talk between EphB and NMDA receptor signaling in synaptic plasticity in mature neurons remains to be determined. Nonetheless, the function of EphA4 in dendritic spine retraction in mature hippocampal neurons prompted us to investigate whether EphA4 is involved

Department of Biochemistry, State Key Laboratory of Molecular Neuroscience and Molecular Neuroscience Center, The Hong Kong University of Science and Technology, Clear Water Bay, Hong Kong, China. Correspondence should be addressed to N.Y.I. (boip@ust.hk).

Received 16 August; accepted 17 November; published online 26 December 2010; doi:10.1038/nn.2715.

in reductions in synaptic strength during homeostatic plasticity, probably acting through interaction with ion channels such as NMDARs or AMPARs.

Using yeast-two hybrid screening, we have identified an interaction between EphA4 and a truncated fragment of anaphase-promoting complex subunit 2 (APC2), a major component of APC in mammals. Here we report that the expression of the GluR1 subunit of the AMPAR was regulated by an APC-dependent proteasomal degradation pathway in neurons. The downregulation of GluR1 and reduction in glutamatergic transmission was mediated by EphA4-APC^{Cdh1}-dependent signaling in response to prolonged elevated activity, revealing a previously undescribed mechanism that underlies the regulation of synaptic strength during homeostatic plasticity.

RESULTS

EphA4 activation downregulates GluR1

To study the role of Eph signaling in the regulation of excitatory glutamatergic transmission, we first examined the effect of ephrin-A1 on the frequency and amplitude of mEPSCs. Consistent with previous results from cultured hippocampal neurons[23], treatment of cultured cortical neurons with ephrin-A1 resulted in a reduction in mEPSC frequency (**Fig. 1a**,**b**), indicative of a decrease in the number of functional synapses. The reduction in mEPSC frequency was specific for ephrin-A1, as we found no similar reduction in neurons treated with Fc- or ephrin-B1 (**Fig. 1a**,**b**). The amplitude of mEPSCs was also reduced in cortical neurons treated with ephrin-A1, which suggests that the expression of AMPARs was decreased at individual synapses (**Fig. 1a**,**c**). Knockdown of EphA4 in neurons by short hairpin RNA (shRNA) abolished the effect of ephrin-A1 on mEPSC amplitude (**Fig. 1d**), indicating that the observed regulation of synaptic strength by ephrin-A is mediated by EphA4.

The reduction in mEPSC amplitude in response to ephrin-A1 prompted us to investigate whether EphA4-dependent signaling regulated the expression of synaptic AMPARs. We treated dissociated hippocampal neurons (19–22 days *in vitro*, DIV) with ephrin-A1 for 24 h and determined the localization and expression of GluR1 and PSD-95. Consistent with the notion that ephrin-A1 treatment leads to a reduction in the number of spines (by ~20%) in dissociated hippocampal neurons[23], we found that the number of PSD-95 clusters was also reduced in neurons treated with ephrin-A1 (by ~25%; **Fig. 2a**,**b**). Treatment of neurons with ephrin-A1 produced a robust reduction in the number of GluR1 clusters (by ~70%; **Fig. 2a**,**b**). Furthermore, ephrin-A1 reduced the number of synaptic GluR1 clusters (by ~65% as indicated by the percentage of PSD-95 clusters that contained GluR1 immunoreactivity; **Fig. 2a**,**c**) as well as the number of GluR1 clusters in the spines (from 57.29 ± 3.93% (Fc) to 39.02 ± 3.69% (ephrin-A1); $P < 0.005$, ephrin-A1 versus Fc, Student's *t*-test), whereas the number of synaptic GluR2 clusters remained relatively unchanged (**Fig. 2c**). To visualize the loss of GluR1 clusters directly after ephrin-A treatment, we performed live cell imaging on cultured neurons expressing GluR1-GFP to monitor the fate of GluR1 puncta[28]. We found that ephrin-A1 enhanced the loss of pre-existing GluR1-GFP clusters, in particular those at dendritic spines (**Fig. 2d**,**e**). Together, these findings suggest that, in addition to reducing the number of functional synapses through elimination of dendritic spines, ephrin-A1 can modulate synaptic strength through an alternative pathway that involves reduced expression of the AMPA receptor subunit GluR1.

We found that ephrin-A1 significantly reduced both the total level and surface expression of GluR1 protein (**Fig. 2f–h**). The reduction in total GluR1 expression was not observed in cultured *EphA4*$^{-/-}$ neurons, indicating that EphA4 is essential for this process (**Fig. 2f**,**g**). EphA4 kinase activity was required for the regulation of GluR1 because expression of EphA4, but not its kinase-dead mutant, resulted in the downregulation of total GluR1 (**Supplementary Fig. 1a**). Moreover, EphA4-dependent signaling specifically downregulated GluR1, and neither GluR2 (**Fig. 2c**,**f**) nor NR1 expression was affected (**Supplementary Fig. 1b**). Consistent with the notion that EphA4 is important for the downregulation of GluR1, we found elevated GluR1 (increased by ~60 ± 19%; $n = 3$, $P < 0.05$; Student's *t*-test) but not elevated NR1 in crude synaptosomal fractions prepared from adult *EphA4*$^{-/-}$ mouse brains (**Fig. 2i**).

EphA4 activation is involved in homeostatic plasticity

Next, we investigated the functional significance of EphA4-dependent downregulation of GluR1 in neurons. Chronic blockade of neuronal activity increases synaptic responses partly through the upregulation of surface AMPAR expression[3]. We therefore explored the possibility that EphA4-dependent regulation of GluR1 expression is involved in the homeostatic response of neurons to chronic bicuculline treatment. Bicuculline enhanced tyrosine phosphorylation and activation of EphA4 in cortical neurons (**Fig. 3a**,**b**),

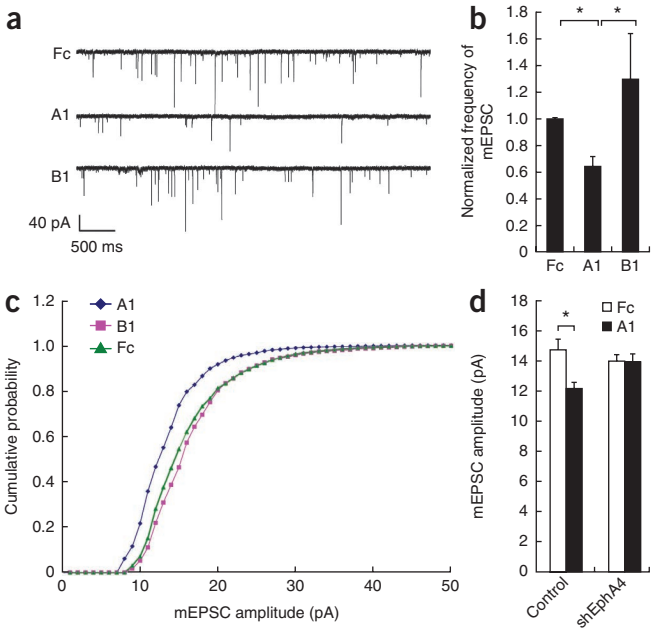

Figure 1 Activation of EphA4 reduces synaptic strength. (**a**–**c**) Cortical neurons (16 DIV) were treated with Fc, ephrin-A1 or ephrin-B1 (5 μg ml^{-1}) for 4 h, and the mEPSC was recorded. (**a**) Representative mEPSC traces. (**b**) Compared to the Fc-treated control, the mean frequency of mEPSCs decreased significantly after treatment with ephrin-A1 but not ephrin-B1. Data are expressed as mean ± s.e.m.; *$P < 0.05$, ANOVA with Student-Newman-Keuls test (4 experiments; >10 neurons recorded from each experiment). (**c**) Cumulative amplitude distribution of mEPSCs in cortical neurons after treatment with Fc, ephrin-A1 or ephrin-B1 for 4 h. There is a leftward shift of cumulative amplitude distribution of mEPSC upon ephrin-A1 treatment. (**d**) Knockdown of EphA4 by shRNA abolished the reduction in mEPSC amplitude triggered by ephrin-A1. Cortical neurons (12–14 DIV) were transfected with GFP and pSUPER-EphA4 shRNA (shEphA4) or pSUPER vector (Control). Neurons at 19–21 DIV were treated with ephrin-A1 for 16 h. The mEPSC was recorded for neurons that expressed GFP. Data are presented as mean ± s.e.m. from three experiments ($n > 10$ neurons from each experiment; *$P < 0.05$, ANOVA followed by Student-Newman Keuls test).

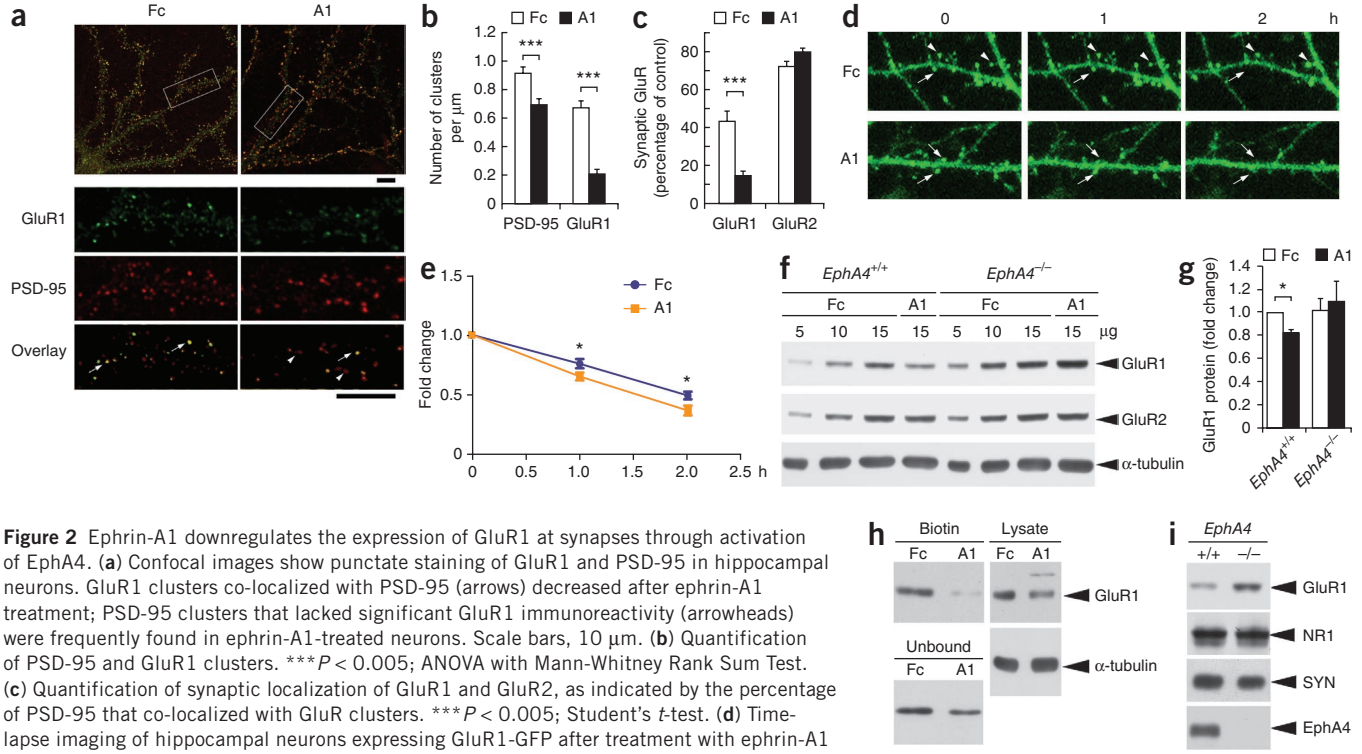

Figure 2 Ephrin-A1 downregulates the expression of GluR1 at synapses through activation of EphA4. (**a**) Confocal images show punctate staining of GluR1 and PSD-95 in hippocampal neurons. GluR1 clusters co-localized with PSD-95 (arrows) decreased after ephrin-A1 treatment; PSD-95 clusters that lacked significant GluR1 immunoreactivity (arrowheads) were frequently found in ephrin-A1-treated neurons. Scale bars, 10 µm. (**b**) Quantification of PSD-95 and GluR1 clusters. ***$P < 0.005$; ANOVA with Mann-Whitney Rank Sum Test. (**c**) Quantification of synaptic localization of GluR1 and GluR2, as indicated by the percentage of PSD-95 that co-localized with GluR clusters. ***$P < 0.005$; Student's *t*-test. (**d**) Time-lapse imaging of hippocampal neurons expressing GluR1-GFP after treatment with ephrin-A1 for 4–6 h. Representative images show that some GluR1 clusters (arrowheads) were more stable, whereas others (arrows) disappeared during the imaging period. (**e**) Quantification of the loss of GluR1-GFP clusters ($n = 11$ for Fc, $n = 12$ for ephrin-A1; *$P < 0.05$, Student's *t*-test). (**f**) Ephrin-A1-mediated reduction in total GluR1 expression depends on EphA4. Cortical neurons prepared from *EphA4*$^{-/-}$ mice or *EphA4*$^{+/+}$ littermates were treated with Fc or ephrin-A1 for 24 h. Different amounts of protein (5–15 µg) were loaded. (**g**) Quantitative analysis of GluR1 protein level (3 experiments; *$P < 0.05$, Student's *t*-test). (**h**) Ephrin-A1 reduced both surface and total GluR1. (**i**) Increased GluR1 in synaptosomes of *EphA4*$^{-/-}$ mouse brains. Crude synaptosomal fractions of whole brains from adult *EphA4*$^{+/+}$ (+/+) or *EphA4*$^{-/-}$ (–/–) mice were prepared, and western blot analysis was performed.

whereas blocking the interaction between ephrin and EphA4 on the cell surface essentially abolished the bicuculline-stimulated activation of EphA4 (**Fig. 3c**,**d**). These results showed that chronic elevation of synaptic activity resulted in the activation of ephrin-EphA4 signaling.

Consistent with previous observations in spinal neurons[29], incubation of cultured cortical neurons with bicuculline for 24 h reduced the total expression of GluR1 (**Fig. 3e**,**f**). The reduction in total GluR1 after chronic bicuculline treatment was abolished in *EphA4*$^{-/-}$ cortical neurons (**Fig. 3e**,**f**). These findings suggest that the decrease in GluR1 caused by prolonged synaptic activity was mediated by EphA4. Chronic elevation of neural activity also significantly reduced the number of GluR1 clusters that colocalized with PSD-95 and the surface GluR1 in cultured hippocampal neurons (**Fig. 3g**,**h** and **Supplementary Fig. 2**), as well as the number of GluR1 clusters at dendritic spines (from 55 ± 3% (control) to 44 ± 1% (bicuculline); $P < 0.005$, Student's *t*-test), which suggests that synaptic GluR1 expression in neurons is reduced upon sustained elevated activity. Notably, the reduction in mEPSC amplitude that is normally observed in control neurons upon chronic bicuculline treatment was essentially abolished in EphA4-knockdown neurons or in neurons that were also treated with EphA4-Fc, which blocks the interaction between endogenous EphA4 and ephrin-A (**Fig. 3i** and **Supplementary Fig. 3**). In addition, treatment of neurons with ephrin-A1 did not result in any further decrease in mEPSC amplitude from that induced by bicuculline (**Fig. 3j**). Together, these data suggest that EphA4-dependent signaling mediates homeostatic scaling in response to sustained elevation of synaptic activity.

EphA4 reduces GluR1 expression through the UPS

Next, we investigated the mechanisms that underlie EphA4-mediated downregulation of GluR1 in neurons. AMPARs are highly dynamic and can cycle between the plasma membrane and intracellular compartments[30,31]. We found that treatment of neurons with chlorpromazine (CPZ), an inhibitor that disrupts clathrin-mediated endocytosis (**Supplementary Fig. 4**), abolished the ephrin-A1-dependent downregulation of GluR1 and reduction in mEPSC amplitude, which suggests that endocytosis is important for EphA4-dependent regulation of synaptic strength. Furthermore, inhibition of the proteasome by MG132 or lactacystin protected GluR1 from EphA4-dependent degradation in transfected HEK293T cells, whereas blockade of lysosomal degradation by chloroquine or NH_4Cl did not affect the degradation of GluR1 triggered by EphA4 (**Fig. 4a**). The proteasome inhibitor MG132 (**Fig. 4b**,**c**) or lactacystin (data not shown) also prevented the ephrin-A1-triggered reduction of GluR1 expression in neurons, indicating that the ubiquitin proteasome pathway is essential for EphA4-dependent degradation of GluR1. Furthermore, the presence of MG132 abolished the reduction in mEPSC amplitude that was caused by ephrin-A1 treatment, thereby verifying that the proteasome is important for reductions in synaptic strength that depend on ephrin-A and EphA4 (**Fig. 4d**).

We then investigated whether ephrin-A1 caused an accumulation of ubiquitinated GluR1 in neurons. Treatment of cortical neurons with ephrin-A1 for 6 h increased the ladder of polyubiquitinated GluR1, as compared with Fc control in the presence of MG132 (**Fig. 4e**). We also detected ubiquitinated GluR1 in synaptosomes from adult rat brain, which suggests that ubiquitination of GluR1 occurs *in vivo*

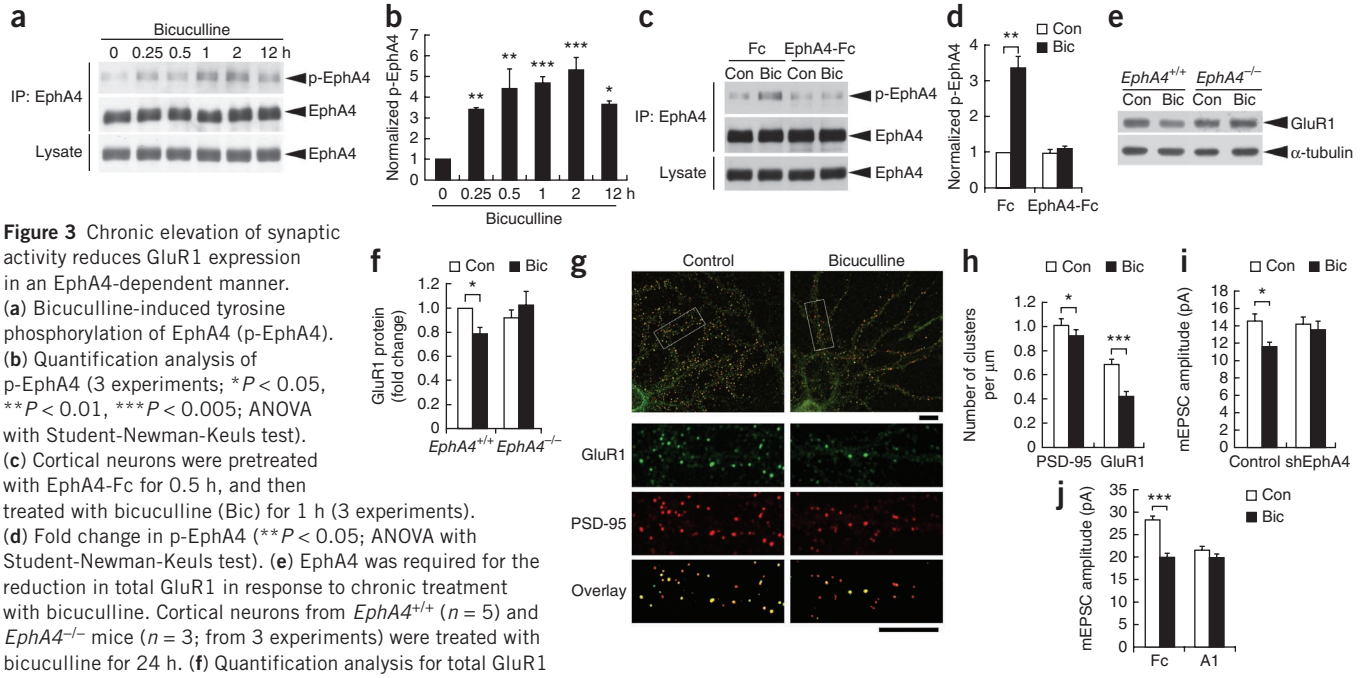

Figure 3 Chronic elevation of synaptic activity reduces GluR1 expression in an EphA4-dependent manner. (**a**) Bicuculline-induced tyrosine phosphorylation of EphA4 (p-EphA4). (**b**) Quantification analysis of p-EphA4 (3 experiments; $*P < 0.05$, $**P < 0.01$, $***P < 0.005$; ANOVA with Student-Newman-Keuls test). (**c**) Cortical neurons were pretreated with EphA4-Fc for 0.5 h, and then treated with bicuculline (Bic) for 1 h (3 experiments). (**d**) Fold change in p-EphA4 ($**P < 0.05$; ANOVA with Student-Newman-Keuls test). (**e**) EphA4 was required for the reduction in total GluR1 in response to chronic treatment with bicuculline. Cortical neurons from *EphA4*$^{+/+}$ ($n = 5$) and *EphA4*$^{-/-}$ mice ($n = 3$; from 3 experiments) were treated with bicuculline for 24 h. (**f**) Quantification analysis for total GluR1 ($P < 0.05$; Student's *t*-test). (**g**–**i**) Bicuculline treatment reduced the number of GluR1 clusters. (**g**,**h**) Hippocampal neurons were treated with bicuculline for 24 h, after which neurons were subjected to immunocytochemical analysis using GluR1 and PSD-95 antibodies. (**g**) Representative confocal images showed punctate staining of GluR1 and PSD-95. (**h**) The number of PSD-95 and GluR1 clusters was reduced after bicuculline treatment (3 experiments; $*P < 0.05$, $***P < 0.001$; ANOVA with Mann-Whitney Rank Sum test). (**i**) EphA4 is required for the reduction of mEPSC amplitude induced by chronic bicuculline treatment. The mEPSC amplitude in shEphA4-transfected cortical neurons after bicuculline treatment (3 experiments; $*P < 0.05$; ANOVA, with Student-Newman-Keuls test). (**j**) Co-treatment with bicuculline and ephrin-A1 does not further reduce the mEPSC amplitude. Cortical neurons were treated with ephrin-A1 (A1), bicuculline or bicuculline with ephrin-A1 (4 experiments; $***P < 0.005$; ANOVA with Student-Newman-Keuls test).

(**Fig. 4f**). Although phosphorylation has been shown to be required for the efficient polyubiquitination of several proteins, EphA4 could not phosphorylate GluR1 (**Supplementary Fig. 5**).

EphA4 interacts with ubiquitin ligase APC^{Cdh1} complex

Next, we investigated whether and how activation of EphA4 promotes the downregulation of GluR1. Using the intracellular domain of EphA4 as bait to perform a yeast two-hybrid screen of a P12 mouse muscle cDNA library[32], we identified a truncated fragment of APC2 as one of the positive clones. APC2 is one of the core units of the ubiquitin ligase APC, which comprises at least 11 core subunits in vertebrates, and the activity of this complex is controlled by the two activators Cdh1 and Cdc20 (ref. 33). Although APC activity was originally identified to be important for controlling cell-cycle

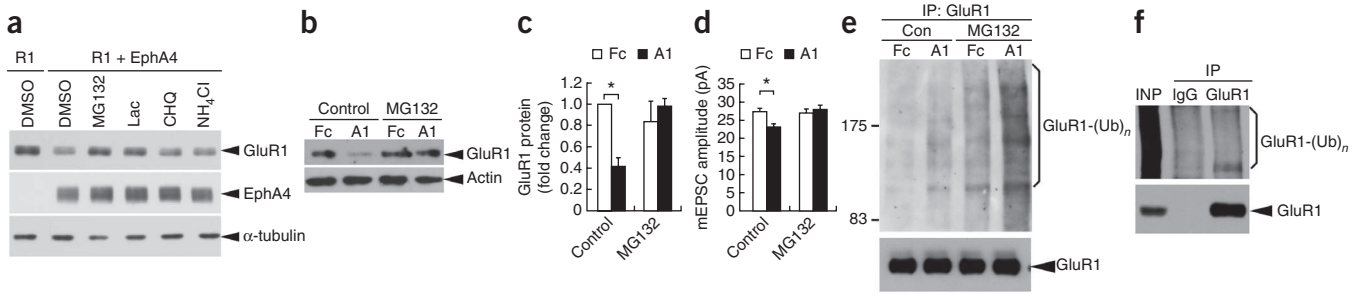

Figure 4 Ephrin-A-EphA4 signaling reduces GluR1 expression by a proteasome-dependent pathway. (**a**,**b**) EphA4-dependent degradation of GluR1 is mediated by a proteasome-dependent pathway. (**a**) HEK293T cells were transfected with GluR1 and EphA4, and were then treated with MG132 (10 µM), lactacystin (Lac, 10 µM), chloroquine (CHQ, 50 µM) or ammonium chloride (NH_4Cl, 20 mM) for 5 h. (**b**) Inhibition of proteasome-mediated degradation abolished the downregulation of GluR1 by ephrin-A1. Cortical neurons were treated with MG132 for 0.5 h before stimulation by ephrin-A1 for 7–16 h in the presence of the inhibitor. (**c**) Quantitative analysis of GluR1 ($n = 4$; $*P < 0.05$, ANOVA with Student-Newman Keuls test). (**d**) Ephrin-A1 reduced mEPSC amplitude through proteasome-mediated degradation. Cortical neurons were treated with MG132 for 0.5 h and then with ephrin-A1 for 16 h. The mEPSC amplitude was measured (≥3 experiments; $*P < 0.05$, ANOVA with Student-Newman Keuls test). (**e**) Ephrin-A1 induced polyubiquitination of GluR1 in neurons. Cultured cortical neurons were treated with MG132 for 0.5 h before treated with ephrin-A1 for 6 h. Whole-cell lysate was immunoprecipitated with GluR1 antibodies, followed by immunoblotting with anti-ubiquitin (Fk2) antibody which recognizes both mono- and polyubiquitinated proteins ($n = 4$). Similar results were observed when anti-polyubiquitin (Fk1) antibodies were used for immunoblotting (data not shown). More polyubiquitinated protein was immunoprecipitated by GluR1 antibodies from neurons treated with ephrin-A1 than from control neurons treated with Fc. (**f**) Ubiquitinated GluR1 was detected in synaptosomes. GluR1 protein was immunoprecipitated from the synaptosomal fractions, followed by western blot analysis using the Fk2 antibody ($n = 3$).

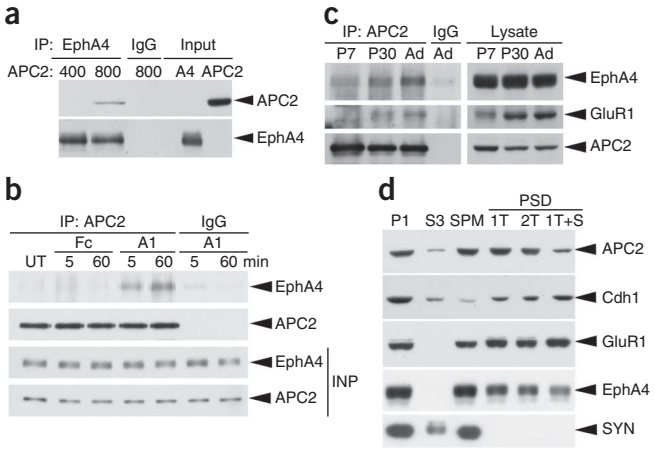

Figure 5 E3 ubiquitin ligase complex APC^{Cdh1} interacts with EphA4. (**a**) EphA4 interacted with APC2. Expression constructs encoding EphA4 and full-length APC2 were overexpressed in HEK293T cells separately. EphA4 was immunoprecipitated using EphA4 antibody and then pulled down by proteinG-Sepharose beads (IgG served as the control). The beads were then incubated with APC2-expressing cell lysate (400 μg or 800 μg as indicated). APC2 protein pull down by EphA4 was examined by western blot analysis. (**b**) Ephrin-A1 increased the interaction between APC2 and EphA4 in neurons. Cortical neurons (14 DIV) were treated with Fc or ephrin-A1 for indicated durations. Lysate was immunoprecipitated with APC2 antibody and immunoblotted with antibodies to EphA4. Similar amounts of protein were subjected to immunoprecipitation for different treatments, as indicated by immunoblotting the lysate (INP) with antibodies to EphA4 and APC2. (**c**) APC2 associated with EphA4 and GluR1 in rat brain *in vivo*. Rat brain homogenate (postnatal day (P)7, P30 and adult (Ad)) was immunoprecipitated with antibodies to APC2 and immunoblotted with antibodies to EphA4, GluR1 or APC2. (**d**) Adult rat brain fractions separated by differential centrifugation and extraction were subjected to western blot analysis for APC2, Cdh1, GluR1 and EphA4. Synaptophysin (SYN) served as the negative control for the different PSD fractions. P1: total brain lysates; S3: cytosolic fraction; SPM: synaptic plasma membrane. SPM was further extracted by Triton X-100 once (PSD 1T), twice (2T), or with Triton X-100 followed by Sarkosyl (1T+S).

transition, the core subunits such as APC2 and its activator Cdh1 are expressed in rat brain and in postmitotic cortical neurons[34] (**Supplementary Fig. 6**). The APC^{Cdh1} complex consists of core APC subunits associated with the activator Cdh1. We confirmed the interaction between EphA4 and full-length APC2 by direct pull-down assay and an overexpression study in HEK293T cells (**Fig. 5a** and **Supplementary Fig. 7a**). Treatment of cultured cortical neurons with ephrin-A1 increased the interaction between APC2 and EphA4 (**Fig. 5b**), indicating that APC^{Cdh1} was recruited to EphA4 in a ligand-dependent manner.

As Cdh1 has been identified as a major APC activator that is expressed in postmitotic neurons[35], we examined whether EphA4 also interacted with Cdh1. Indeed, Cdh1 was co-immunoprecipitated with activated EphA4 when they were co-expressed in HEK293T cells (**Supplementary Fig. 7b**). Furthermore, EphA4 and GluR1 were co-immunoprecipitated with APC2 in postnatal and adult rat brain homogenates (**Fig. 5c**), indicating that a complex of EphA4, GluR1 and APC^{Cdh1} exists *in vivo*. Consistent with the observation that the APC complex is linked to synaptic functions in *C. elegans*[15], we found that Cdh1 and APC2 were concentrated in the detergent-resistant postsynaptic fractions of adult rat brain, which suggests that there is a tight association between APC^{Cdh1} and postsynaptic proteins (**Fig. 5d**).

APC^{Cdh1} ubiquitinates and downregulates GluR1

Degradation of protein substrates by APC requires the interaction of its substrate with one of its activators, which then targets the substrate to the APC core for ubiquitination[33]. Therefore, we investigated whether APC can ubiquitinate and degrade GluR1 through the recognition of GluR1 by Cdh1. We co-transfected GluR1, Cdh1 and His-myc-tagged ubiquitin into HEK293T cells. We then incubated the lysate of GluR1-overexpressing cells with Ni-NTA agarose beads, which pulled down polyubiquitinated proteins. GluR1 was present in the ubiquitin pull-down fraction and appeared as multiple bands above the size of GluR1, indicating that GluR1 was polyubiquitinated when ectopically expressed in HEK293T cells (**Fig. 6a**). Although expression of Cdh1 increased the polyubiquitination of GluR1, expression of a mutant form of Cdh1 (ΔWD40), which lacks the substrate-binding WD40 domain and therefore acts as a dominant-negative to inhibit ubiquitination of proteins[36], completely abolished the polyubiquitination of GluR1 (**Fig. 6a**). These findings confirm the importance of Cdh1 in APC-mediated ubiquitination of GluR1.

Cdh1 recruits the substrate to core APC for degradation through its direct binding to the degradation motifs on the substrate. We found that Cdh1 interacted preferentially with the extracellular N-terminal region of GluR1 (**Fig. 6b**). To verify that GluR1 could be recognized by APC^{Cdh1}, we searched for degradation motifs (that is, destruction box (D-box RxxLxxxxN/D/E), A-box motif (QRVL) or KEN-box motif (KEN)) in the primary sequence of GluR1. We identified three potential degradation motifs (amino acids 43–51, RFALSQLTE; amino acids 126–134, RPELQEALI; and amino acids 159–162, QRVL) in the N-terminal region of GluR1. We speculate that the extracellular N-terminal region of GluR1 interacts with components of the APC ubiquitin ligase complex, as has been suggested for the degradation of NMDARs[37]; however, the precise underlying mechanism requires further investigation. Nonetheless, we generated a full-length GluR1 mutant (3M) with mutations in all three degradation motifs, and found that simultaneous mutation of these motifs abolished the direct interaction between Cdh1 and GluR1 (**Fig. 6c**). These findings suggest that Cdh1 recognized the degradation motifs of GluR1 and recruited GluR1 to core APC. We then tested whether ubiquitination of GluR1 by APC^{Cdh1} led to the downregulation of GluR1. Co-expression of Cdh1 with GluR1 significantly reduced both the surface and total expression of GluR1 in transfected HEK293T cells (**Fig. 6d**), which suggests that Cdh1 enhanced the degradation of GluR1.

To confirm that GluR1 underwent APC^{Cdh1}-dependent degradation, we performed a pulse-chase assay using S^{35} labeling to trace the fate of total GluR1 upon Cdh1 overexpression. We found that whereas Cdh1 enhanced the degradation of GluR1 in HEK 293T cells, MG132 could partially inhibit the loss of GluR1 (**Fig. 6e**), which suggests that GluR1 underwent Cdh1-dependent degradation. To investigate whether GluR1 was targeted by APC^{Cdh1} through its recognition by Cdh1, we overexpressed in HEK293T cells expression constructs of Cdh1 and different GluR1 mutants with mutations on single degradation motifs. Mutation of the D-box motif (amino acids 43–51 (D-43M) or 126–134 (D-126M)) but not of the A-box motif (A-159M) abolished the degradation of GluR1 by Cdh1 (**Fig. 6f**). The D box sequence (amino acids 43–51) was not conserved in the GluR2 subunit. This finding, together with the observation that EphA4 interacts with GluR1 but not with GluR2 (**Supplementary Fig. 8**), might account for why EphA4 activation results in specific degradation of GluR1 (**Fig. 2c**,**d**,**h**).

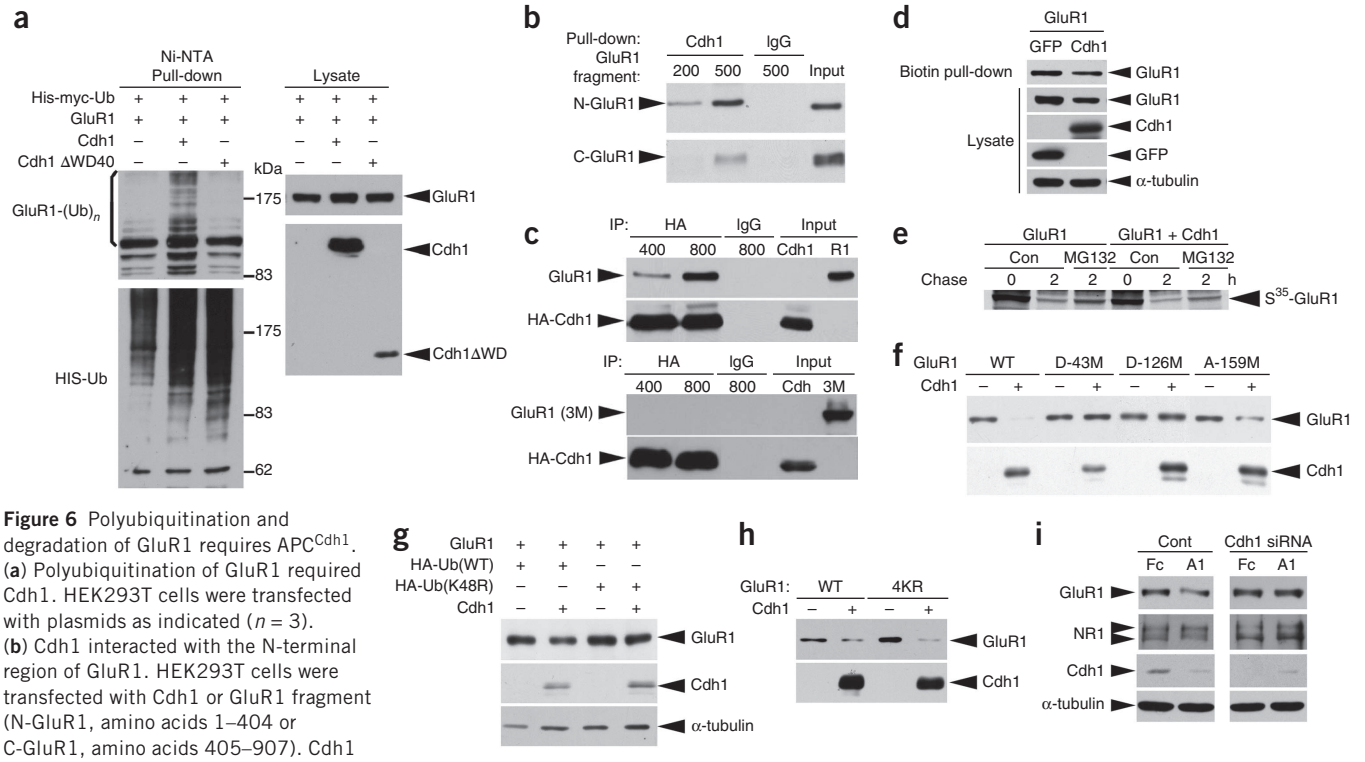

Figure 6 Polyubiquitination and degradation of GluR1 requires APC^{Cdh1}. (**a**) Polyubiquitination of GluR1 required Cdh1. HEK293T cells were transfected with plasmids as indicated ($n = 3$). (**b**) Cdh1 interacted with the N-terminal region of GluR1. HEK293T cells were transfected with Cdh1 or GluR1 fragment (N-GluR1, amino acids 1–404 or C-GluR1, amino acids 405–907). Cdh1 protein was pulled down by Cdh1 antibody, and was then incubated with cell lysate expressing GluR1 fragments (200 or 500 μg). Input, 10 μg. (**c**) Degradation motifs on GluR1 are important for GluR1-Cdh1 interaction. HEK293T cells were transfected with Cdh1 and GluR1 or its 3M mutant. (**d**) Cdh1 reduced surface and total GluR1 in HEK293T cells. (**e**) Blockade of proteasome-dependent degradation partially inhibits the Cdh1-dependent degradation of GluR1. HEK293T cells overexpressing GluR1 or GluR1 with Cdh1 were pulse-labeled with [^{35}S]-methionine and chased for 2 h. (**f**) The integrity of D-box motifs on GluR1 was required for Cdh1-dependent degradation of GluR1 in HEK293T cells; GluR1 (WT) or its single point mutants (D-43M, D-126M or A-159M). (**g**) Expression of ubiquitin mutant (K48R) inhibited the Cdh1-dependent degradation of GluR1. (**h**) Simultaneous mutation of lysine residues 831, 837, 840 and 886 to arginine (4KR) could not stabilize the expression of GluR1 when co-transfected with Cdh1. (**i**) Knockdown of Cdh1 inhibited the ephrin-A1-dependent reduction of GluR1. Cortical neurons were transfected with Cdh1 siRNA and then treated with ephrin-A1. The reduced expression of Cdh1 after EphA4 activation may be due to auto-degradation as Cdh1 is a target of APC^{Cdh1}[48].

To further study the effect of ubiquitination on GluR1 stability, we transfected HEK293T cells with GluR1, Cdh1 and either wild-type ubiquitin or its dominant-negative form (K48R), in which Lys48 was mutated to arginine. Lys48-linked polyubiquitinated proteins undergo 26S proteasome-dependent degradation, whereas expression of the K48R mutant terminates ubiquitin chain production and prevents protein degradation[38]. Co-transfection of wild-type ubiquitin and Cdh1 led to a reduction in GluR1 expression, whereas overexpression of the ubiquitin K48R mutant resulted in stabilization of GluR1 (**Fig. 6g**), further confirming that GluR1 undergoes 26S-proteasomal dependent degradation. The lysine specificity is determined by E2 enzymes. Whereas different E2s including UbcH5, UbcH10 and E2-25K exert distinct actions on APC-dependent formation of the ubiquitin chain[39], the identity of E2s that collaborate with APC^{Cdh1} in neurons requires further investigation. We attempted to identify the lysine residues on GluR1 that are responsible for ubiquitination. However, mutation of the four lysine residues at the cytoplasmic region of GluR1 could not inhibit its degradation by Cdh1 (ref. 14; **Fig. 6h**). Therefore, the identity of specific lysine residue(s) on mammalian GluR1 that are required for ubiquitination awaits further studies.

EphA4 downregulates synaptic strength through APC^{Cdh1}

To confirm that the ubiquitin ligase activity of APC^{Cdh1} is essential for ephrin-A-stimulated degradation of GluR1 in neurons, we knocked down Cdh1 in cultured cortical neurons by shRNA, which abolished the degradation of GluR1 after ephrin-A1 stimulation (**Fig. 6i**). Inhibition of Cdh1 function by expression of the Cdh1 ΔWD40 mutant also abolished the reduction in mEPSC amplitude produced by treatment with ephrin-A1 (**Fig. 7a**,**b**). Re-expression of shRNA-resistant Cdh1 construct in Cdh1 knockdown neurons could restore the ephrin-A-mediated reduction in mEPSC amplitude, indicating that the reduction in synaptic strength caused by ephrin-A required Cdh1 (**Fig. 7c**,**d**). Together with the observation that ephrin-A1 reduced total GluR1 expression in a proteasome-dependent manner (**Fig. 4b**), these results support the notion that ephrin-A1 stimulation recruits GluR1 and the APC^{Cdh1} complex to activated EphA4, which then leads to polyubiquitination and proteasome-dependent degradation of GluR1 and thereby reduces synaptic strength.

To verify our hypothesis that EphA4 scaled down synaptic strength through APC^{Cdh1} in response to chronic elevation of synaptic activity, we investigated whether Cdh1-dependent signaling was involved in the regulation of GluR1 expression during homeostatic plasticity. Either transfection with the Cdh1 ΔWD40 mutant or knockdown of Cdh1 prevented the bicuculline-induced reduction in mEPSC amplitude (**Fig. 7e–h**), suggesting that Cdh1-dependent protein degradation by the proteasome is essential in homeostatic plasticity. Together, our findings provide evidence that chronic elevation of synaptic activity reduces synaptic strength by triggering the proteasome-dependent degradation of GluR1 through a pathway that requires EphA4 and APC^{Cdh1}.

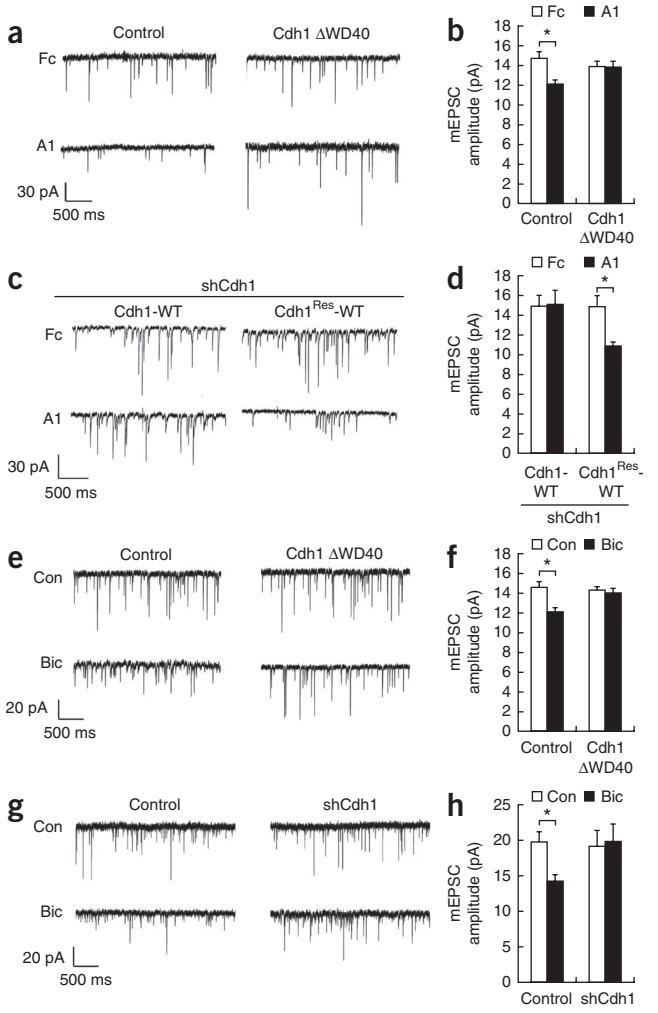

Figure 7 Reduction of synaptic strength by ephrin-A1 or chronic treatment of bicuculline depends on APC^{Cdh1}-dependent proteasome degradation pathway. (**a**,**b**) Expression of Cdh1 ΔWD40 mutant abolished the reduction in synaptic strength after ephrin-A1 treatment. Cortical neurons (14–16 DIV) were transfected with Cdh1 ΔWD40 and GFP, and then treated at 20–22 DIV with ephrin-A1 for 16–24 h. (**a**) Representative traces. (**b**) Quantification of mEPSC amplitude after ephrin-A1 treatment (from three independent experiments; $*P < 0.05$, ANOVA with Student-Newman Keuls test). (**c**,**d**) Expression of shRNA-resistant Cdh1 in Cdh1-depleted neurons restored the ephrin-A1-dependent reduction in mEPSC amplitude. Cortical neurons were transfected with shCdh1 together with the Cdh1-WT or shRNA-resistant Cdh1 expression constructs, then treated with ephrin-A1. (**c**) Representative traces. (**d**) Quantification of mEPSC amplitude (from three experiments; $*P < 0.05$, ANOVA with Student-Newman Keuls test). (**e**–**h**) Inhibition of Cdh1 or knockdown of Cdh1 in neurons abolished the reduction in mEPSC amplitude after treatment with bicuculline for 16–24 h. Cortical neurons were transfected with Cdh1 ΔWD40 and GFP (**e**,**f**) or pSUPER-Cdh1 shRNA (shCdh1) or pSUPER vector (Control) together with GFP (**g**,**h**), and then treated with bicuculline (Bic) for 16–24 h. (**e**,**g**) Representative traces. (**f**,**h**) Quantification of mEPSC amplitude upon bicuculline treatment. Data are expressed as mean ± s.e.m. (>10 neurons recorded from each experiment, ≥3 experiments; $*P < 0.05$, ANOVA with Dunn's test).

DISCUSSION

There is emerging evidence that ephrin and Eph receptors are important for regulating the synaptic functions of mature neurons in the CNS. Although previous studies have reported abnormal LTP and LTD in knockout mice that lack specific ephrins or Eph receptors[20], it is not clear how ephrin and Eph-mediated signaling leads to changes in synaptic strength during different forms of plasticity. One possible mechanism involves the regulation of activity-dependent morphological changes in dendritic spines[22–25]. Much less is known about whether ephrin and Eph receptor signaling can regulate the expression of specific postsynaptic proteins such as ion channels, which would represent an alternative mechanism for directly modulating synaptic transmission. Here, we report that EphA4 activation downregulated GluR1 expression and mEPSC amplitude in neurons. We further show that the reduction of GluR1 level and mEPSC amplitude was mediated by an APC and Cdh1–dependent proteasomal pathway upon EphA4 activation. Instead of having a permissive role in regulating the basal turnover of GluR1, EphA4 mediated the downregulation of GluR1 during chronic elevation of synaptic activity. The reduction in mEPSC amplitude was completely abolished in Cdh1-deficient cortical neurons, indicating that EphA4-APC^{Cdh1} has a crucial role in regulating excitatory synaptic transmission during homeostatic plasticity. To our knowledge, these findings provide the first evidence that EphA4 and APC^{Cdh1} signaling are involved in homeostatic plasticity in response to elevated synaptic activity, and identify a function for EphA4 signaling in modifying the molecular composition of excitatory synapses. Together with previous studies on the role of EphA4 in dendritic spine retraction[22,23], our findings lead us to propose that EphA4 is a key negative regulator of synaptic strength, and that it has a crucial role in scaling down synaptic responses after a chronic increase in synaptic activity.

Our study shows that EphA4 is involved in homeostatic plasticity after prolonged elevation of synaptic activity, but the cellular response to bicuculline treatment might not be identical to the response to ephrin treatment. Notably, bicuculline treatment appears to mainly result in downregulation of mEPSC amplitude, whereas activation of EphA4 led to a reduction in both the frequency and amplitude of mEPSCs accompanied by reduced spine density[22,23]. Moreover, the expression of GluR1 but not GluR2 is specifically downregulated after ephrin stimulation, but the specific AMPAR subunit reduced after chronic elevation of synaptic activity remains controversial. As multiple signaling pathways regulate homeostatic plasticity[40], it is possible that other signaling pathways in addition to EphA4 are involved in regulating synaptic strength. Nonetheless, by knocking down EphA4 expression or culturing neurons from EphA4 knockout mice, we have shown that EphA4 is essential for downregulating synaptic GluR1 expression and reducing mEPSC amplitude upon prolonged bicuculline treatment (**Fig. 3e**–**j**). These findings, together with the observation that ephrin-A1 treatment did not decrease mEPSC amplitude below that induced by bicuculline (**Fig. 3j**), support the notion that EphA4-dependent signaling is crucial for homeostatic scaling induced by sustained elevation of synaptic activity.

The APC^{Cdh1}-dependent reduction in mEPSC amplitude after bicuculline treatment suggests that downregulation of GluR1 depends on the activity of ubiquitin ligase. This finding is consistent with an earlier study showing that ubiquitin-mediated degradation of postsynaptic proteins is bidirectionally regulated after chronic elevation or blockade of synaptic activity[13]. Prolonged changes in neuronal activity trigger a homeostatic response that involves changes in the abundance of synaptic AMPARs, which mediate most excitatory neurotransmission[2,3,29]. It is well accepted that chronic exposure to bicuculline promotes endocytosis of AMPARs, which could account for the homeostatic reduction of mEPSC amplitude[2–4,41,42].

Notably, the agonist-induced endocytosis of AMPARs depends on the ubiquitin proteasome pathway[10], suggesting that AMPARs themselves are not the target of ubiquitin-mediated degradation. Rather, there are AMPAR-interacting proteins that undergo polyubiquitination and subsequent degradation, thereby regulating the surface expression of AMPARs. This notion is supported by findings that NMDA triggers AMPAR endocytosis via proteasome-dependent degradation of PSD-95 (ref. 17). By contrast, a recent study suggested that the abundance of AMPARs can be regulated by endocytosis as well as by proteasome-dependent pathways, and that this regulation is important for maintaining intracellular sodium homeostasis in neurons[18]. As EphA4 is tyrosine phosphorylated and endocytosed shortly after stimulation by its ligand[23], and blockade of clathrin-mediated endocytosis inhibits the ephrinA-mediated reduction in GluR1 expression and mEPSC amplitude, it is likely that endocytosis is important for the EphA4-dependent downregulation of GluR1. Because of the lack of suitable antibodies for double-immunofluorescence staining, we cannot currently investigate where activated EphA4 and GluR1 are colocalized. It will be interesting to further examine whether these receptors diffuses laterally as a complex on the cell surface or interact after endocytosis.

Studies on *Drosophila* neuromuscular junctions and *C. elegans* have identified APC and SCF complexes as the ubiquitin ligases that regulate the expression of postsynaptic glutamate receptors[15,16]. There are many ubiquitin ligases in mammals, and despite the unequivocal importance of the UPS in different forms of neuronal plasticity, the identity of the specific ubiquitin ligases that are involved in the degradation of postsynaptic proteins remains elusive. Here we provide compelling evidence that APC^{Cdh1} is involved in the downregulation of GluR1. First, APC2 is associated with GluR1 and EphA4 in the brain *in vivo*; second, APC2 is recruited to EphA4 in a ligand-dependent manner; third, co-expression of APC activator Cdh1 in HEK293T cells enhances the downregulation of GluR1; fourth, the expression of Cdh1 ΔWD40 mutant or the knockdown of Cdh1 blocks the reduction in mEPSC amplitude induced by ephrin-A1; and finally, inhibition of Cdh1 function abolishes the reduction in mEPSC amplitude that is induced by chronic elevation of synaptic activity. The participation of other ubiquitin ligases in regulating synaptic strength has begun to be elucidated. For example, the F-box protein Fbx2, a component of the SCF complex, interacts with NMDARs and this interaction leads to degradation of NR1 (ref. 37). The SCF ubiquitin ligase is also implicated in the degradation of the postsynaptic RapGAP SPAR after chronic treatment with picrotoxin[43,44]. The E3 ubiquitin ligase Mdm2 is involved in the degradation of PSD-95 after NMDA stimulation[17], and another ubiquitin ligase Parkin has been shown to regulate transmission at excitatory synapses[45]. A large repertoire of postsynaptic proteins undergoes regulated proteasome-dependent degradation during homeostatic plasticity[13], and the substrate specificity of different ubiquitin ligases at the postsynaptic density remains to be determined. The expression of homeostatic plasticity might also occur at presynaptic terminals[46,47]. It will be important to elucidate the role of ubiquitin-mediated proteasome degradation and the identities of the ubiquitin ligase(s)that are involved in regulating the turnover of presynaptic proteins.

METHODS

Methods and any associated references are available in the online version of the paper at http://www.nature.com/natureneuroscience/.

Note: Supplementary information is available on the Nature Neuroscience website.

ACKNOWLEDGMENTS

We thank P. Bartlett for *EphA4*$^{-/-}$ mice, R. Huganir for GluR1 antibodies and the GluR1 4KR mutant expression construct, R. Malinow for the GluR1-GFP construct, J. Chamberlain for the mouse muscle cDNA library, L. Shi, W. Chau, K. Kong, X.-N. Li, W. Fang, E. Cheung, B. Butt and C. Kwong for technical assistance, and members of the Ip laboratory for discussions. This study was supported in part by the Research Grants Council of Hong Kong SAR (HKUST, 6444/06M, 661007, 661109, 1/06C and 6/CRF/08), the Area of Excellence Scheme of the University Grants Committee (AoE/B-15/01) and the Hong Kong Jockey Club. N.Y. Ip and K.-O. Lai were recipients of the Croucher Foundation Senior Research Fellowship and Croucher Foundation Fellowship, respectively.

AUTHOR CONTRIBUTIONS

N.Y.I. supervised the project. A.K.Y.F., K.-W.H., W.-Y.F., K.-O.L. and N.Y.I. designed the experiments. K.-W.H., W.-Y.F., Y.C. and K.-O.L. conducted the majority of experiments. A.K.Y.F., K.-W.H., W.-Y.F., Y.C., K.-O.L. and N.Y.I. did the data analyses. J.X. designed and did the data analyses on the electrophysiology experiment and C.S. performed electrophysiology experiment. A.K.Y.F., K.-O.L. and N.Y.I. wrote the manuscript.

COMPETING FINANCIAL INTERESTS

The authors declare no competing financial interests.

Published online at http://www.nature.com/natureneuroscience/.
Reprints and permissions information is available online at http://www.nature.com/reprintsandpermissions/.

1. Turrigiano, G.G. The self-tuning neuron: synaptic scaling of excitatory synapses. *Cell* **135**, 422–435 (2008).
2. Turrigiano, G.G., Leslie, K.R., Desai, N.S., Rutherford, L.C. & Nelson, S.B. Activity-dependent scaling of quantal amplitude in neocortical neurons. *Nature* **391**, 892–896 (1998).
3. Shepherd, J.D. *et al.* Arc/Arg3.1 mediates homeostatic synaptic scaling of AMPA receptors. *Neuron* **52**, 475–484 (2006).
4. Stellwagen, D. & Malenka, R.C. Synaptic scaling mediated by glial TNF-α. *Nature* **440**, 1054–1059 (2006).
5. Bingol, B. & Schuman, E.M. Synaptic protein degradation by the ubiquitin proteasome system. *Curr. Opin. Neurobiol.* **15**, 536–541 (2005).
6. Yi, J.J. & Ehlers, M.D. Ubiquitin and protein turnover in synapse function. *Neuron* **47**, 629–632 (2005).
7. Haglund, K., Di Fiore, P.P. & Dikic, I. Distinct monoubiquitin signals in receptor endocytosis. *Trends Biochem. Sci.* **28**, 598–603 (2003).
8. Ciechanover, A. Intracellular protein degradation: from a vague idea thru the lysosome and the ubiquitin-proteasome system and onto human diseases and drug targeting. *Cell Death Differ.* **12**, 1178–1190 (2005).
9. Zhao, Y., Hegde, A.N. & Martin, K.C. The ubiquitin proteasome system functions as an inhibitory constraint on synaptic strengthening. *Curr. Biol.* **13**, 887–898 (2003).
10. Patrick, G.N., Bingol, B., Weld, H.A. & Schuman, E.M. Ubiquitin-mediated proteasome activity is required for agonist-induced endocytosis of GluRs. *Curr. Biol.* **13**, 2073–2081 (2003).
11. Jordan, B.A. *et al.* Identification and verification of novel rodent postsynaptic density proteins. *Mol. Cell. Proteomics* **3**, 857–871 (2004).
12. Li, K.W. *et al.* Proteomics analysis of rat brain postsynaptic density. Implications of the diverse protein functional groups for the integration of synaptic physiology. *J. Biol. Chem.* **279**, 987–1002 (2004).
13. Ehlers, M.D. Activity level controls postsynaptic composition and signaling via the ubiquitin-proteasome system. *Nat. Neurosci.* **6**, 231–242 (2003).
14. Burbea, M., Dreier, L., Dittman, J.S., Grunwald, M.E. & Kaplan, J.M. Ubiquitin and AP180 regulate the abundance of GLR-1 glutamate receptors at postsynaptic elements in *C. elegans*. *Neuron* **35**, 107–120 (2002).
15. Juo, P. & Kaplan, J.M. The anaphase-promoting complex regulates the abundance of GLR-1 glutamate receptors in the ventral nerve cord of *C. elegans*. *Curr. Biol.* **14**, 2057–2062 (2004).
16. van Roessel, P., Elliott, D.A., Robinson, I.M., Prokop, A. & Brand, A.H. Independent regulation of synaptic size and activity by the anaphase-promoting complex. *Cell* **119**, 707–718 (2004).
17. Colledge, M. *et al.* Ubiquitination regulates PSD-95 degradation and AMPA receptor surface expression. *Neuron* **40**, 595–607 (2003).
18. Zhang, D. *et al.* Na,K-ATPase activity regulates AMPA receptor turnover through proteasome-mediated proteolysis. *J. Neurosci.* **29**, 4498–4511 (2009).
19. Pasquale, E.B. Eph-Ephrin bidirectional signaling in physiology and disease. *Cell* **133**, 38–52 (2008).
20. Klein, R. Bidirectional modulation of synaptic functions by Eph/ephrin signaling. *Nat. Neurosci.* **12**, 15–20 (2009).
21. Deininger, K. *et al.* The Rab5 guanylate exchange factor Rin1 regulates endocytosis of the EphA4 receptor in mature excitatory neurons. *Proc. Natl. Acad. Sci. USA* **105**, 12539–12544 (2008).

22. Murai, K.K., Nguyen, L.N., Irie, F., Yamaguchi, Y. & Pasquale, E.B. Control of hippocampal dendritic spine morphology through ephrin-A3/EphA4 signaling. *Nat. Neurosci.* **6**, 153–160 (2003).
23. Fu, W.Y. *et al.* Cdk5 regulates EphA4-mediated dendritic spine retraction through an ephexin1-dependent mechanism. *Nat. Neurosci.* **10**, 67–76 (2007).
24. Penzes, P. *et al.* Rapid induction of dendritic spine morphogenesis by trans-synaptic ephrinB-EphB receptor activation of the Rho-GEF kalirin. *Neuron* **37**, 263–274 (2003).
25. Henkemeyer, M., Itkis, O.S., Ngo, M., Hickmott, P.W. & Ethell, I.M. Multiple EphB receptor tyrosine kinases shape dendritic spines in the hippocampus. *J. Cell Biol.* **163**, 1313–1326 (2003).
26. Dalva, M.B. *et al.* EphB receptors interact with NMDA receptors and regulate excitatory synapse formation. *Cell* **103**, 945–956 (2000).
27. Takasu, M.A., Dalva, M.B., Zigmond, R.E. & Greenberg, M.E. Modulation of NMDA receptor-dependent calcium influx and gene expression through EphB receptors. *Science* **295**, 491–495 (2002).
28. Wierenga, C.J., Ibata, K. & Turrigiano, G.G. Postsynaptic expression of homeostatic plasticity at neocortical synapses. *J. Neurosci.* **25**, 2895–2905 (2005).
29. O'Brien, R.J. *et al.* Activity-dependent modulation of synaptic AMPA receptor accumulation. *Neuron* **21**, 1067–1078 (1998).
30. Malinow, R. AMPA receptor trafficking and long-term potentiation. *Philos. Trans. R. Soc. Lond. B Biol. Sci.* **358**, 707–714 (2003).
31. Bredt, D.S. & Nicoll, R.A. AMPA receptor trafficking at excitatory synapses. *Neuron* **40**, 361–379 (2003).
32. Cheng, K. *et al.* Pctaire1 interacts with p35 and is a novel substrate for Cdk5/p35. *J. Biol. Chem.* **277**, 31988–31993 (2002).
33. Castro, A., Bernis, C., Vigneron, S., Labbe, J.C. & Lorca, T. The anaphase-promoting complex: a key factor in the regulation of cell cycle. *Oncogene* **24**, 314–325 (2005).
34. Konishi, Y., Stegmuller, J., Matsuda, T., Bonni, S. & Bonni, A. Cdh1-APC controls axonal growth and patterning in the mammalian brain. *Science* **303**, 1026–1030 (2004).
35. Gieffers, C., Peters, B.H., Kramer, E.R., Dotti, C.G. & Peters, J.M. Expression of the CDH1-associated form of the anaphase-promoting complex in postmitotic neurons. *Proc. Natl. Acad. Sci. USA* **96**, 11317–11322 (1999).
36. Kraft, C., Vodermaier, H.C., Maurer-Stroh, S., Eisenhaber, F. & Peters, J.M. The WD40 propeller domain of Cdh1 functions as a destruction box receptor for APC/C substrates. *Mol. Cell* **18**, 543–553 (2005).
37. Kato, A., Rouach, N., Nicoll, R.A. & Bredt, D.S. Activity-dependent NMDA receptor degradation mediated by retrotranslocation and ubiquitination. *Proc. Natl. Acad. Sci. USA* **102**, 5600–5605 (2005).
38. Lim, K.L. *et al.* Parkin mediates nonclassical, proteasomal-independent ubiquitination of synphilin-1: implications for Lewy body formation. *J. Neurosci.* **25**, 2002–2009 (2005).
39. Matyskiela, M.E., Rodrigo-Brenni, M.C. & Morgan, D.O. Mechanisms of ubiquitin transfer by the anaphase-promoting complex. *J. Biol.* **8**, 92 (2009).
40. Pozo, K. & Goda, Y. Unraveling mechanisms of homeostatic synaptic plasticity. *Neuron* **66**, 337–351 (2010).
41. Lissin, D.V. *et al.* Activity differentially regulates the surface expression of synaptic AMPA and NMDA glutamate receptors. *Proc. Natl. Acad. Sci. USA* **95**, 7097–7102 (1998).
42. O'Brien, R.J., Lau, L.F. & Huganir, R.L. Molecular mechanisms of glutamate receptor clustering at excitatory synapses. *Curr. Opin. Neurobiol.* **8**, 364–369 (1998).
43. Seeburg, D.P., Feliu-Mojer, M., Gaiottino, J., Pak, D.T. & Sheng, M. Critical role of CDK5 and Polo-like kinase 2 in homeostatic synaptic plasticity during elevated activity. *Neuron* **58**, 571–583 (2008).
44. Ang, X.L., Seeburg, D.P., Sheng, M. & Harper, J.W. Regulation of postsynaptic RapGAP SPAR by Polo-like kinase 2 and the SCFbeta-TRCP ubiquitin ligase in hippocampal neurons. *J. Biol. Chem.* **283**, 29424–29432 (2008).
45. Helton, T.D., Otsuka, T., Lee, M.C., Mu, Y. & Ehlers, M.D. Pruning and loss of excitatory synapses by the parkin ubiquitin ligase. *Proc. Natl. Acad. Sci. USA* **105**, 19492–19497 (2008).
46. Murthy, V.N., Schikorski, T., Stevens, C.F. & Zhu, Y. Inactivity produces increases in neurotransmitter release and synapse size. *Neuron* **32**, 673–682 (2001).
47. Burrone, J., O'Byrne, M. & Murthy, V.N. Multiple forms of synaptic plasticity triggered by selective suppression of activity in individual neurons. *Nature* **420**, 414–418 (2002).
48. Listovsky, T. *et al.* Mammalian Cdh1/Fzr mediates its own degradation. *EMBO J.* **23**, 1619–1626 (2004).

ONLINE METHODS

Constructs, chemicals, antibodies and animals. Full-length mouse APC2 was subcloned into expression vector pcDNA3 for overexpression experiments. Cdh1 siRNA was purchased from Santa Cruz Biotechnology. Chloroquine, chlorpromazine (CPZ), cycloheximide, MG132 and lactacystin (Lac) were purchased from Calbiochem. Antibodies specific for EphA4, HA and HIS were purchased from Santa Cruz Biotechnology. Antibodies specific for GluR1 and GluR2 were purchased from Chemicon, NR1 from BD Biosciences, PSD-95 from BioAffinity Reagents, ubiquitin (Fk2) and poly-ubiquitin (Fk1) from Biomol. GluR1 4KR expression construct and antibodies to the N-terminal region of GluR1 were gifts from R. Huganir (John Hopkins University). APC2-specific antibodies were raised against recombinant proteins encoding the APC2 C-terminal region. Ephrin-A1 and B1 were purchased from R&D Systems whereas Fc and goat antibodies to human Fc were supplied by Jackson ImmunoResearch. All animal procedures were conducted in accordance with the Guidelines of the Animal Care Facility of the Hong Kong University of Science and Technology (HKUST) and were approved by the Animal Ethics Committee in HKUST.

Yeast two-hybrid screen. Complementary DNA encoding cytoplasmic region of EphA4 (EphA4-IC) was subcloned into the yeast GAL4 DNA-binding vector pAS2-1 (Clontech) to construct GAL4bd-EphA4-IC, which was used as bait in the yeast two-hybrid screen. The yeast two-hybrid screen was performed following the Matchmaker two-hybrid screen protocol (Clontech). EphA4-IC was used as a bait to screen a mouse muscle cDNA library (a gift from J. Chamberlain, University of Washington) that was constructed in the GAL4 transcriptional activation vector (pACT2) as described[32]. Yeast strain Y190 was transformed with the bait and the library plasmids and transformants were selected on SD-Trp-Leu-His plus 10-mM 3-AT plates. β-galactosidase activity of His^+ colonies was assayed by filter assay.

Cell culture, transfection and ephrin clustering. HEK293T cells were cultured in Dulbecco's modified Eagle's medium (Invitrogen) supplemented with 10% heat-inactivated FBS plus antibiotics. HEK293T cells were transfected with pcDNA3 expression constructs using lipofectamine/plus reagent (Invitrogen). Primary cortical and hippocampal neurons were prepared from embryonic day 18–19 rat embryos as described[23]. Briefly, cortical neurons (5×10^6 per plate) were plated on 100-mm culture dishes coated with poly-D-lysine (12.5 μg ml^{-1}; Sigma). Cortical neurons were fed with Neurobasal medium (Invitrogen) supplemented with 2% B27 and 5 mM L-glucose (Invitrogen). Rat hippocampal neurons were seeded on 18-mm coverslips coated with poly-D-lysine (50 μg ml^{-1}) at a density of 0.5×10^5 per 18-mm coverslip for immunocytochemical analysis; or at a density of 2×10^5 per 35-mm dish with central coverglass (Matek Corporation) for live-cell imaging. Cortical neurons at 12–16 DIV were transfected with different plasmids plus EGFP using calcium phosphate precipitation[49]. Cortical neurons from day 18 embryos of $EphA4^{+/+}$ or $EphA4^{-/-}$ mice were plated on two 35-mm culture dishes. Ephrin-B1-Fc and ephrin-A1-Fc (R&D Systems) were pre-clustered with goat anti-human Fc antibody (Jackson ImmunoResearch Labs) in a ratio of 1:2 and 1:4.5, respectively, as described[23], and incubated at room temperature for 1 h before use. Neurons were treated with ephrin or Fc at 5 μg ml^{-1} and bicuculline at 20 μM. To examine the effect of proteasomes on ephrin-A-treated neurons, neurons were treated with MG132 at 10 μM.

Pull-down, co-immunoprecipitation and western blot analysis. HEK293T cells and cultured cortical neurons were lysed in lysis buffer A (20 mM Tris, pH 7.6, 150 mM NaCl, 1 mM EDTA, 1 mM EGTA, 1 mM NaF, 0.5% Nonidet P-40). Rat brain was homogenized in lysis buffer B (50 mM Tris, pH 8, 150 mM NaCl, 2 mM EGTA, 1 mM dithiothreitol, 1% Nonidet P-40, 0.25% sodium deoxycholate, 50 mM NaF) with various protease inhibitors. Western blot analysis was performed as described[23]. For direct pull-down assay, lysates were prepared from HEK293T cells overexpressing specific protein, immunoprecipitated with the corresponding antibody, followed by incubation with protein G-Sepharose. The protein G-Sepharose beads were then incubated with cell lysate of HEK293T cells that expressed the protein of interest. The pull-down protein was then examined by western blot analysis. Co-immunoprecipitation of HEK293T cell lysates was performed in lysis buffer A. Five-hundred μg of HEK293T cell lysates was incubated with the corresponding antibodies (1 μg) at 4 °C overnight and then incubated with 50 μl of protein G-Sepharose at 4 °C for 1 h. The samples were washed with buffer A and resuspended in SDS sample buffer. Co-immunoprecipitated proteins were detected by western blot analysis.

Cell-surface biotinylation and ubiquitination assay. Twenty-four hours after transfection, HEK293T cells were washed twice in ice-cold Dulbecco's phosphate buffer (DPBS) and subsequently incubated with 0.5 mg ml^{-1} EZ-link-sulfo-NHS-Biotin (Pierce) on ice for 0.5 h. Biotin was removed, the reaction was quenched by the addition of 5 mM glycine in DPBS, and the cells were washed three times in ice-cold DPBS. Cells were then scraped in 0.1 ml of radioimmunoprecipitation assay (RIPA) buffer (1% Triton X-100, 1% sodium deoxycholate, 0.1% SDS, 150 mM NaCl, 10 mM sodium phosphate, 2 mM EDTA and 0.2% sodium vanadate) supplemented with protease inhibitors and solubilized at 4 °C for 0.5 h. Non-solubilized material was removed by centrifugation at 16,000*g* for 10 min. Biotinylated proteins were separated from non-biotinylated proteins by incubation with UltraLink Plus Immobilized Streptavidin Gel (Pierce) at 4 °C for 2 h. Beads were washed with the lysis buffer, and the adsorbed proteins were then eluted with SDS sample buffer. To examine the polyubiquitination of GluR1 in neurons, ~2–3 mg lysate of cortical neurons after ephrin treatment in the presence of MG132 was collected. The lysate was then immunoprecipitated with GluR1 antibodies. Western blot analysis using anti-ubiquitin (Fk2) antibodies or anti-polyubiquitin (Fk1) antibodies was performed.

Pulse chase assay. Transfected HEK293T cells were washed with methionine-free DMEM twice, and incubated in the same medium for 30 min. The cells were then pulse-labeled by incubation in methionine-free DMEM containing 50 μCi ml^{-1} [^{35}S]-methionine (PerkinElmer) for 0.5 h, and the medium was then replaced with DMEM + 10% HIFBS containing 2 mM methionine together with MG132 and cycloheximide (10 μg ml^{-1}) for the indicated chase time. The cells were washed twice with ice-cold DPBS before lysed in RIPA buffer, and the cell lysate was subjected to immunoprecipitation with HA antibody (Santa Cruz), followed by protein G-sepharose beads. The samples were subjected to SDS–PAGE and analyzed by autoradiography.

Immunocytochemical analysis and confocal microscopy. To examine the endogenous expression of GluR1 and PSD-95, the low density neurons were fixed with 4% paraformaldehyde/5% sucrose at room temperature for 5 min followed with methanol at −20 °C for 15 min. Immunostaining was performed as described[50]. Briefly, the neurons were incubated with PSD-95 antibody (1:500) and GluR1 antibody (1:1,000) in GDB buffer at 4 °C overnight, then washed with phosphate buffer and incubated with corresponding secondary antibody at room temperature for 1 h. For surface staining of the GluR1, cortical neurons were incubated with antibodies against the extracellular domain of GluR1 in cultured medium at 37 °C for 5 min as described[50]. To quantify the spines that contained GluR1 clusters, the neurons were transfected with GFP plasmid, and then stained as described[23]. For image acquisition, the cells were washed and mounted in ProLong antifade reagent (Invitrogen) and images were acquired by Olympus Fluoview FV1000 confocal microscope with a 60× oil-immersion objective using *z*-serial scanning mode. Images from the same experiment were obtained using identical acquisition settings and the image analyses were performed with Metamorph software (Meta image series 7.5, Universal Imaging). Live imaging of hippocampal neurons expressing GluR1-GFP was performed by Nikon A1 Confocal microscopy with the 37 °C incubator system (Tokai Hit). For image acquisition, 8–12 serial stack images covering a depth of ~12–20 μm were collected using a 60× objective.

Quantification and statistical analysis. The images were quantified in a double-blinded manner as described[23]. Briefly, cultured neurons were imaged and examined under the same acquisition parameters. A stack of images (*z* step, 0.5 μm) of 5–6 layers was collected using a 60× objective. For each condition, 15–20 neurons from 3 independent experiments were analyzed using MetaMorph software (Universal Imaging Corp.). For quantification, two dendrite segments from each neuron were analyzed. The outline of dendrites was manually traced. The basal threshold values for the background of all images in each experiment were measured. The average of these threshold values was then applied to all images in the same experiment. To measure the density of clusters in spines or colocalization of staining, the images were first thresholded to include the clusters

doi:10.1038/nn.2715

with intensity of twofold above the signal of adjacent dendrite. Total number of clusters and dendrite length were measured automatically, and colocalized staining was determined when thresholded puncta from two channels overlapped.

Densitometric quantification of protein band intensity was performed using the NIH Image J program. Statistical analysis was performed, where appropriate, using Student's *t*-test or ANOVA followed by tests as indicated in the figure legends. All experiments were performed at least three times except those specifically indicated.

Electrophysiology. For miniature EPSC recordings, cortical neurons at ~16–20 DIV were used. Whole-cell patch-clamp recordings were made at room temperature with external solution containing (in mM) 110 NaCl, 5 KCl, 2 $CaCl_2$, 0.8 $MgCl_2$,10 HEPES and 10 D-glucose (pH 7.4) and an internal solution containing (in mM) 135 $CsCl_2$, 10 HEPES, 2 $MgCl_2$, 4 NaATP, 0.4 NaGTP and 0.5 EGTA (pH 7.2)[23]. 200 μM picrotoxin was included in the external solution to block GABAergic inhibitory postsynaptic potentials and 0.5 μM TTX to prevent action potential-evoked EPSCs. For miniature EPSC recordings, cells were held at −70 mV. Pipette resistances for these experiments were typically 3–5 MΩ and series resistances 15–20 MΩ. Only recording epochs in which series and input resistances varied by <10% were analyzed. At least ten neurons were subjected to recording for each experiment. Data were presented as mean ± s.e.m. from at least three experiments.

49. Sala, C. *et al.* Regulation of dendritic spine morphology and synaptic function by Shank and Homer. *Neuron* **31**, 115–130 (2001).
50. Sala, C. *et al.* Inhibition of dendritic spine morphogenesis and synaptic transmission by activity-inducible protein Homer1a. *J. Neurosci.* **23**, 6327–6337 (2003).